Extreme N_2O accumulation in the coastal oxygen minimum zone off Peru

Annette Kock[1], Damian L. Arévalo-Martínez[1], Carolin R. Löscher[2,3], Hermann W. Bange[1]

[1]GEOMAR Helmholtz Centre for Ocean Research Kiel, Düsternbrooker Weg 20, 24105 Kiel, Germany

[2] Institute of General Microbiology, Christian-Albrechts University Kiel, Am Botanischen Garten 1-9, 24118 Kiel, Germany

[3]Now at: GEOMAR Helmholtz Centre for Ocean Research Kiel, Düsternbrooker Weg 20, 24105 Kiel, Germany

Correspondence to: Annette Kock, akock@geomar.de

Abstract

Depth profiles of nitrous oxide (N_2O) were measured during six cruises to the upwelling area and oxygen minimum zone (OMZ) off Peru in 2009 and 2012/2013, covering both the coastal shelf region and the adjacent open ocean. N_2O profiles displayed a strong sensitivity towards oxygen concentrations. Open ocean profiles with distances to the shelf break larger than the first baroclinic Rossby radius of deformation showed a transition from a broad maximum close to the equator to a double-peak structure south of 5°S where the oxygen minimum was more pronounced. Maximum N_2O concentrations in the open ocean were about 80 nM. A linear relationship between ΔN_2O and apparent oxygen utilization (AOU) could be found for all measurements within the upper oxycline, with a slope similar to studies in other oceanic regions. In contrast, N_2O profiles close to the shelf revealed a much higher variability, and N_2O concentrations higher than 100 nM were often observed. The highest N_2O concentration measured at the shelf was ~850 nM. Due to the extremely sharp oxygen gradients at the shelf, N_2O maxima occurred in very shallow water depths of less than 50 m. In the coastal area, a linear relationship between ΔN_2O and AOU could not be observed as extremely high ΔN_2O values were scattered over the full range of oxygen concentrations. The data points that showed the strongest deviation from a linear ΔN_2O/AOU relationship also showed signals of intense nitrogen loss. These results indicate that the coastal upwelling at the Peruvian coast and the subsequent strong remineralization in the water column causes conditions that lead to extreme N_2O accumulation, most likely due to the interplay of intense mixing and high rates of remineralization which lead to a rapid switching of the OMZ waters between anoxic and oxic conditions. This, in turn, could trigger incomplete denitrification or pulses of increased nitrification with extreme N_2O production.

1 Introduction

Nitrous oxide (N_2O) acts as a strong atmospheric greenhouse gas and contributes substantially to the stratospheric ozone depletion (IPCC, 2013; WMO, 2011). The ocean is a major source for N_2O as it is naturally produced in the water column (Ciais et al., 2013; Bange, 2008). While in large parts of the surface ocean N_2O concentrations are close to saturation, high emissions of N_2O have been observed in upwelling areas where subsurface waters enriched in N_2O are transported to the surface (e.g. Nevison et al., 2004). The global distribution of N_2O in the ocean is closely linked to the oceanic oxygen distribution, and particularly high supersaturations are found in upwelling areas which overlay pronounced oxygen minimum zones (OMZ), e.g. in the Arabian Sea (Bange et al., 2001) or in the eastern South Pacific Ocean (Charpentier et al., 2010).

These OMZs are key regions for marine nitrogen (N) cycling where active N loss via canonical denitrification and anaerobic ammonium oxidation (anammox) takes place. Particularly in areas where the OMZ is fuelled by high export production, high rates of denitrification and anammox, but also other N transformation processes, such as nitrification, have been observed (Hu et al., 2015; Kalvelage et al., 2013). Oceanic N_2O is mainly produced by nitrification and denitrification, and the interplay of these processes governs the N_2O distribution in OMZs (Bange, 2008).

The relationship between N_2O and oxygen concentrations in the ocean in often described by comparing excess N_2O (ΔN_2O) and the apparent oxygen utilization (AOU). As nitrification is one major process accompanying the remineralization of organic matter, a positive correlation between the excess N_2O (ΔN_2O) and the apparent oxygen utilization (AOU) is often interpreted as an indication for nitrification as the main N_2O production pathway (e.g. Walter et al., 2006; Forster et al., 2009). Nitrification can either be performed by bacteria (Arp and Stein, 2003) or archaea (Walker et al., 2010). Recent studies indicate that archaea may dominate marine N_2O production under oxic conditions (Löscher et al., 2012; Santoro et al., 2011). The production mechanisms and environmental controls of archaeal N_2O production are subject to ongoing research, however (Stieglmeier et al., 2014).

An increase in the ΔN_2O/AOU ratio at low oxygen concentrations has been observed in several studies in different oceanic areas with reduced oxygen concentrations (Ryabenko et al., 2012; Upstill-Goddard et al., 1999; De Wilde and Helder, 1997). This could be explained by several processes: During nitrification, N_2O can either be produced as a side product from the oxidation of ammonium to nitrite, or from the reduction of nitrite to N_2O, a process known as nitrifier-denitrification (Stein, 2011). Nitrifier-denitrification has been identified as an important production pathway of N_2O at low oxygen concentrations and may thus be responsible for the increased N_2O production under these conditions (Ni et al., 2014). An increase in the N_2O yield of nitrification has indeed been observed in laboratory experiments with bacterial (Goreau et al., 1980) and archaeal ammonium oxidizers (Löscher et al., 2012). The extent to which ammonium oxidation or the nitrifier-denitrification pathway are responsible for N_2O production is yet not well determined (Ostrom et al., 2000; Ni et al., 2014), particularly for archaeal nitrification (Löscher et al., 2012; Santoro et al., 2011; Stieglmeier et al., 2014).

Additional N_2O production from denitrification has also been proposed as a potential mechanism leading to an increased ΔN_2O/AOU at low oxygen concentrations (e.g. Farías et al., 2009; Ji et al., 2015). During denitrification, the canonical reduction of nitrate to molecular nitrogen, N_2O evolves as an intermediate product. Denitrification is stimulated by the supply of organic carbon or hydrogen sulfide (Chang et al., 2014; Dalsgaard et al., 2014; Galan et al., 2014), and active denitrification is restricted to suboxic to anoxic conditions (e.g. Firestone et al., 1980; Dalsgaard et al., 2014).Depending on the environmental conditions, N_2O production or consumption due to denitrification can be observed in the environment. There has been evidence that N_2O consumption is more sensitive to trace amounts of oxygen than N_2O production. This could lead to N_2O accumulation when oxygen is present in low concentrations (Tiedje, 1988). Exceptionally high N_2O concentrations off the West Indian Coast were thus associated with an increased N_2O production from denitrification during transient oxygen concentrations (Naqvi et al., 2000). In a recent study it was furthermore shown that N_2O production from denitrification could be stimulated by H_2S addition (Dalsgaard et al., 2014) which could indicate a coupling between N_2O production and sulfur cycling.

At oxygen concentrations below a threshold value of 4 - 10 µM, (Nevison et al., 2003; Ryabenko et al., 2012; Cornejo and Farias, 2012), consumption of N_2O in the water column is observed, which leads to a breakdown in the previously described positive ΔN_2O/AOU relationship. The exact oxygen concentration at which N_2O consumption starts is not yet well determined, however (Cornejo and Farias, 2012; Zamora et al., 2012). N_2O consumption has been associated with denitrification as the only known process to consume N_2O in OMZ waters (Cornejo and Farias, 2012). Although rate measurements only rarely detected active denitrification in the water column of the ETSP (Kalvelage et al., 2013; Hamersley et al., 2007; Thamdrup et al., 2006), the widespread N_2O consumption in the OMZ core is an indicator for active denitrification (Farias et al., 2007).

There is a strong indication that at low oxygen concentrations nitrification and denitrification may take place in close proximity (Kalvelage et al., 2011), and the N_2O production and consumption under these conditions are strongly influenced by the interaction of both processes (Ji et al., 2015). Measurements of N_2O consumption rates in the eastern tropical North Pacific Ocean (ETNP) furthermore provided evidence for a rapid N_2O cycling, although depth profiles of N_2O seemed to be relatively invariant over time (Babbin et al., 2015). These quasi-stable conditions may be disturbed by rapid changes in the environmental conditions.

The eastern tropical South Pacific Ocean (ETSP) harbors one of the four major eastern boundary upwelling systems (EBUS): alongshore trade winds induce offshore Ekman transport of the surface water masses which leads to strong coastal upwelling off Peru and Chile (Chavez and Messié, 2009). While year-round upwelling and high primary productivity can be observed along the Peruvian coast (Messie et al., 2009), the highest upwelling intensity can be observed during austral winter, whereas primary production seems to be higher during autumn and spring (Pennington et al., 2006), which may be caused by nutrient and light limitation during phases of intense upwelling (Echevin et al., 2008).

The region is influenced by strong seasonal and interannual variability caused by the influence of Equatorial Kelvin waves and the El Niño Southern Oscillation (ENSO). ENSO could cause the interruption of the upwelling during El Niño events (Dewitte et al., 2012; Graco et al., 2016). While the OMZ core is largely unaffected by ENSO, a deepening of the upper oxycline and the re-oxygenation of the Peruvian shelf due to the propagation of coastal trapped waves can be observed (Gutierrez et al., 2008).

The ETSP is characterized by one of the largest and most intense OMZs in the oceans, extending from the Peruvian shelf about 1000 km offshore with a maximum thickness of more than 600 m (Fuenzalida et al., 2009). It is located in the shadow zone of large ocean current systems which leads to a sluggish ventilation and long residence times of waters within the OMZ (Karstensen et al., 2008). Equatorial current bands such as the Equatorial Undercurrent (EUC) and the Southern Subsurface Countercurrents (SSCC) supply waters to the ETSP which leads to slightly elevated oxygen concentrations in the northern part of our study area, with minimum oxygen concentrations of 10 - 20 µM (Stramma et al., 2010), whereas oxygen concentrations below 3 µM are common in the OMZ core south of 5°S (Paulmier et al., 2006). The equatorial current bands also feed the poleward Peru-Chile Undercurrent (PCUC) which is the main source for waters upwelled along the coast (Montes et al., 2010; Chaigneau et al., 2013) and which transports Equatorial Subsurface Water (ESSW) southward. During its spreading, the ESSW is subject to oxygen depletion and mixing with surrounding water masses, e.g. the Antarctic Intermediate Water (AAIW) below and the Eastern South Pacific Intermediate Water (ESPIW) which originates from the South (Wyrtki, 1967; Chaigneau et al., 2013). Mixing of different water masses in the upwelling zone creates a distinct coastal water mass which is called Cold Coastal Water (CCW) (Pietri et al., 2013).

High primary production and high remineralization rates in the underlying waters lead to a further drawdown in subsurface oxygen concentrations to near-depleted conditions (Karstensen et al., 2008). Active N loss is observed in large parts of the OMZ which is reflected in a pronounced secondary nitrite maximum and a strong nitrogen deficit in the OMZ core (Codispoti et al., 1986). The OMZ furthermore frequently extends over large parts of the Peruvian shelf where sulfidic conditions within the water column can be observed (Schunck et al., 2013).

Here we present N_2O measurements in the water column off Peru from six measurement campaigns in the ETSP. Previous depth profile measurements in this area showed a pronounced double-peak structure off South Peru which merged into a broad maximum north of 5°N (Cornejo and Farias, 2012; Ryabenko et al., 2012). Surface N_2O measurements off Peru furthermore revealed extraordinarily high emissions from the Peruvian shelf area which corresponded to extremely high surface and subsurface N_2O concentrations (Arévalo-Martínez et al., 2015).

2 Methods

In total, 146 depth profiles (0-~4200 m) of N_2O were measured on two cruises between December 2008 and February 2009 (M77-3 & M77-4) and four cruises between October 2012 and March 2013 (M90 - M93) to the upwelling area and the adjacent open ocean off Peru onboard the German research vessel Meteor. The Southern Oscillation Indices (http://www.ncdc.noaa.gov/teleconnections/enso/indicators/soi/) from 2008/2009 and 2012/2013 did not indicate the presence of an El Niño event during our measurement campaigns and similar conditions between both measurement campaigns could be expected. The locations of the sampled stations are shown in Fig. 1. While the M77-4 and M90 cruises mainly covered the open ocean area, the M77-3 and M91-M93 cruises mainly took place in the Peruvian shelf area. The work was part of the German DFG collaborative research project (SFB) 754 (https://www.sfb754.de/) and the BMBF project SOPRAN (Surface Ocean PRocesses in the ANthropocene, www.sopran.pangaea.de). The N_2O data set described here has been archived in MEMENTO, the MarinE MethanE and NiTrous Oxide database (https://memento.geomar.de) (Kock and Bange, 2015).

Triplicate samples were taken from 10 L Niskin bottles mounted on a rosette water sampler or a pump-CTD (M77-3) in 25 ± 0.11 mL (M77-3 & M77-4) and 20 ± 0.14 mL (M90 - M93) opaque glass vials and sealed with butyl rubber stoppers and aluminum caps, thereby avoiding the inclusion of air bubbles.

Samples were treated with 0.2 mL (M77-3 & M77-4) and 0.05 mL (M90 - M93) of a saturated mercuric chloride solution directly after the sampling to inhibit microbial N_2O production or consumption. The samples were either analyzed onboard (M77-3 & M77-4, M91, partly M90 & M93) within a few days or shipped to GEOMAR by air freight for later analysis (M92, partly M90 & M93). Samples that were shipped to Germany were additionally sealed with paraffin wax and stored upside down to avoid the formation of air bubbles in the samples due to temperature and pressure changes during transportation.

Samples were analyzed using a static equilibration method: 10 mL helium (99.9999%, AirLiquide, Düsseldorf, Germany) was manually injected into each vial which was equipped with a second syringe to collect the overflowing water. Vials with added headspace were vigorously shaken for about 20 s and allowed to equilibrate at ambient temperature for a minimum of two hours. A subsample of the equilibrated headspace was manually injected into a GC-ECD system (Hewlett-Packard 5890 Series II, Agilent Technologies, Santa Clara, CA, USA), equipped with a 6' 1/8" packed column (molsieve, 5Å, W. R. Grace & Co.-Conn., Columbia, MY). The GC was operated at 190 °C, using argon/methane (95%/5%, ECD purity, AirLiquide, Düsseldorf, Germany) as carrier gas at a flow rate of 30 mL min^{-1}.

The GC was calibrated on a daily basis with a minimum of 2 (M77-3 & M77-4) or 4 (M90 - M93) different standard gas mixtures (N_2O in synthetic air, Deuste-Steininger GmbH, Mühlhausen, Germany and Westfalen AG, Münster, Germany). Standard gases were either injected as pure gas or further diluted with helium (1:3, 1:1 or 3:1) to obtain additional standard gas concentrations. Our standard gases were calibrated against NOAA primary standards at the Max Planck Institute for Biogeochemistry in Jena, Germany, if the standard gas concentrations were within the calibration range of the NOAA gases. Gases with N_2O concentrations outside the NOAA calibration range were internally calibrated using an LGR N_2O/CO analyzer (Los Gatos Research, Mountain View, CA, USA), which was proven to have a linear response and minimal drift within the calibration range (Arévalo-Martínez et al., 2013). The N_2O concentration in the samples was calculated according to Walter et al. (2006) using the solubility function of Weiss and Price (1980). The average precision of the measurements, calculated as median standard deviation from triplicate measurements, was 0.7 nM.

ΔN_2O was calculated as the difference between the in-situ concentration $[N_2O]_w$ and the equilibrium concentration $[N_2O]_{eq}$:

$$\Delta N_2O = [N_2O]_w - [N_2O]_{eq} \qquad (1)$$

We used the contemporary atmospheric mixing ratio measured at Cape Grim, Tasmania (http://agage.mit.edu/data/agage-data) for the calculation of $[N_2O]_{eq}$. This calculation underestimates the N_2O excess in subsurface waters which have been isolated from the surface for a long time as it does not account for the increase in the atmospheric mixing ratio since the beginning of the industrial revolution (Freing et al., 2009). The use of the contemporary N_2O mixing ratio of 2013 would lead to a maximum ~17% overestimate of $[N_2O]_{eq}$, thus leading to only a small error compared to the maximum N_2O concentrations measured in our study, and the use of the contemporary atmospheric mixing ratio still allows a qualitative analysis of the ΔN_2O/AOU relationship in order to investigate the formation and consumption processes of N_2O.

The potential temperature of the water parcel at a certain depth was calculated using the Gibbs Seawater Oceanographic Toolbox (McDougall and Barker, 2011).

Oxygen concentrations were measured either with a Seabird (M77-3 & M77-4: SBE-5; M90-M93: SBE 43) oxygen sensor (Sea-Bird Electronics, Bellevue, WA, USA) mounted on the CTD rosette or from 100 mL discrete samples taken from the Niskin bottles and analyzed using the Winkler titration method (Grasshoff et al., 1999). The oxygen sensor was calibrated against the Winkler measurements.

Recent studies using highly sensitive STOX (Switchable Trace amount Oxygen) sensors for oxygen measurements indicate that measurements with conventional oxygen sensors that are calibrated against Winkler measurements may be biased towards higher concentrations at near-zero oxygen conditions. Thamdrup et al. (2012) therefore argued that anoxic conditions are prevalent in the core of the Peruvian OMZ where oxygen concentrations of several µM have been found using the conventional Winkler-calibrated measurements. As STOX sensor measurements were not available for all measurement campaigns presented here, the minimum oxygen measurements reported here from the core of the OMZ (3-5 µM) should be considered as an overestimation.

The Apparent Oxygen Utilization (AOU) was calculated from the oxygen concentrations $[O_2]_w$ using the CSIRO SeaWater library, version 3.2 (http://www.cmar.csiro.au/datacentre/ext_docs/seawater.htm) to calculate oxygen saturation $[O_2]_{eq}$:

$$AOU = [O_2]_w - [O_2]_{eq} \qquad (2)$$

Nutrient samples ($[NO_3^-]$, $[NO_2^-]$, $[PO_4^{3-}]$, $[NH_4^+]$) from the CTD rosette were analyzed onboard following the nutrient analysis methods according to Hansen et al. (1999). Samples taken from the pump-CTD during M77-3 were stored at -20°C and shipped to Germany for later analysis. N' was calculated as a measure for the nitrogen deficit from the nitrate ($[NO_3^-]$), nitrite ($[NO_2^-]$) and phosphate ($[PO_4^{3-}]$) concentrations as follows (Altabet et al., 2012):

$$N' = ([NO_3^-] + [NO_2^-]) - 16[PO_4^{3-}] \qquad (3)$$

To distinguish between coastal and open ocean stations we calculated the distance of each station from the continental slope (2000 m isobath) and used the first baroclinic Rossby radius of deformation as described by Chelton et al. (1998) as threshold distance for stations that were influenced by coastal upwelling.

3 Results

3. 1 Spatial distribution of oxygen, nutrients and N_2O

The distribution of oxygen, nitrite and N_2O along an offshore section between 16°S and 2°N at 86° W from the M77-4 cruise in 2009 and the M90 cruise in 2012 is shown in Figure 2; a coastal cross-shelf section along 12°S with the distribution of oxygen, nutrients, N' and N_2O is shown in Figure 3 and selected depth profiles of oxygen, N_2O and potential density (σ_θ) as well as nitrate, nitrite, ammonium and N' are shown in Figure 4.

Along 86° W, a similar distribution of oxygen, nitrite and N_2O was observed during M77-4 and M90. Oxygen and N_2O profiles concentrations were close to saturation in the mixed layer. The mixed layer depth increased from below 20 m in the northern part of the section to more than 100 m south of 15 °S. Below the mixed layer, a sharp oxycline with a decrease to oxygen concentrations below 10 µM was observed south of 5°S, whereas in the northern part of the section, below the mixed layer oxygen concentrations only decreased to ~100 µM in the upper 200 m and further dropped to concentrations ~10 µM between 200 and 500 m. Minimum oxygen concentrations in the water column increased towards the north from below 5 µM south of 5° S to ~10 µM at the equator.

The nitrite distribution revealed a primary maximum at the base of the mixed layer with maximum nitrite concentrations below 1.5 µM. This primary maximum is frequently observed in the ocean and is usually associated with nitrification (Codispoti and Christensen, 1985). South of 5° S, a secondary nitrite maximum was observed within the OMZ where oxygen concentrations fell below 5 µM. Nitrite concentrations in the secondary maximum reached up to ~4 µM.

Along the cross-shelf section at 12°S, the upper OMZ boundary significantly became shallower towards the coast as a signal of upwelling, with a well oxygenated mixed layer of ~50 m in the open ocean and a mixed layer depth of less than 5 m on the shelf. Oxygen was strongly undersaturated in the surface waters on the shelf as a result of upwelling of waters from the underlying OMZ (Fig. 4). Elevated phosphate concentrations in the surface waters at the coast also reflected the upwelling on the shelf, whereas nitrate was depleted in the water column and the surface waters close to the coast, which was also reflected in very low N' values at the inshore stations (Fig. 3). A primary and secondary nitrite maximum at the base of the mixed layer and in the OMZ core was observed throughout the cross-shelf section, but both maxima were much more pronounced on the shelf than in the deep waters (Fig. 3).

The N_2O distribution along 86°W could be divided into two different regimes: north of 5 °S, a broad N_2O maximum with concentrations of ~60 nM coincided with the depth of the oxygen minimum, whereas in the southern part of the section, the N_2O profiles revealed a double-peak structure with a sharp N_2O maximum in the upper and lower oxycline and N_2O depletion in the OMZ core, also coinciding with the secondary nitrite maximum. This shape of N_2O profiles has been observed in OMZ regions before (e.g. Law and Owens, 1990; Cohen and Gordon, 1978). The transition from profiles with a broad N_2O peak to a double-peak structure coincided with the decrease in the minimum oxygen concentrations towards the South. N_2O depletion was observed in profiles were oxygen concentrations dropped below ~5 µM and nitrite accumulation was observed.

Compared to the offshore waters, the N_2O distribution on the shelf and in the adjacent waters showed a much larger variability. N_2O depletion was in fact observed at oxygen concentrations below 5 µM, too. While several N_2O profiles revealed a shape similar to the offshore profiles, an overall characteristic shape could not be identified, however: profiles with a subsurface N_2O maximum in the oxycline were observed as well as profiles with multiple maxima or a surface N_2O maximum (Fig. 4). While N_2O concentrations in the offshore waters did not exceed 80 nM, N_2O concentrations above 100 nM were frequently observed at the shelf. Several profiles showed an extreme N_2O accumulation with concentrations above 500 µM (maximum ~850 nM) (Fig. 4). The location and shape of the N_2O maxima in the different profiles was highly variable, which resulted in a very patchy distribution of N_2O in the water column (Fig. 3).

3.2 N_2O in different water masses of the ETSP

The water mass distribution in our dataset agrees well with the data presented by Pietri et al. (2014) (Fig. 5). Due to the larger area covered by our measurements our data showed a broader scattering, but we could identify the same water masses in our data: below 500 m, both the coastal and the offshore profiles carry relatively fresh (S~34.8) and cool (T_{pot}~5°C) Antarctic Intermediate Water (AAIW) (Pietri et al., 2014) that carried relatively high oxygen and ΔN_2O values which corresponded to the secondary N_2O maximum in the lower oxycline. Shallower subthermocline waters are covered by the Equatorial Subsurface Water (ESSW) (S~34.8 – 35.2, T_{pot}~9-14 °C) (Wyrtki, 1967). This water mass carried very low oxygen down to concentrations, while ΔN_2O values showed either a maximum or N_2O depletion in this water mass, which reflects the strong sensitivity of net N_2O consumption to variations in the oxygen concentration.

Waters with low salinities (~34.7), relatively high oxygen concentrations and potential temperatures between 10°C and 15°C can be traced back to Eastern South Pacific Intermediate Water (ESPIW) (Schneider et al., 2003). ΔN_2O values within this water mass were between 20 and 30 nM. Pietri et al. (2014) identified narrow patches of ESPIW below the thermocline about ~100 km offshore. We hardly found this water mass in the coastal data, but it is likely mixed with the ESSW and surface waters on the shelf, where it contributes to the formation of Cold Coastal Water (CCW) (Pietri et al., 2014). CCW with S ~35.1 and T_{pot} ~15.5°C was prevalent over the shelf and could only be identified in the coastal data as it is directly related to the coastal upwelling. Offshore surface data were associated with Subtropical Surface Water (STSW) with salinities above 35.0 and temperatures higher than 17° C (Pietri et al., 2013), while surface waters at the coast showed properties that resulted from the warming of the CCW and the mixing with STSW.

Very variable ΔN_2O values were associated with the CCW and its related surface waters, and nearly all data points that showed extreme N_2O accumulation fell within these waters. This indicates that the extremely high N_2O concentrations were locally produced in the upwelling area, as none of the source water masses for the upwelling carried similarly high ΔN_2O values.

3.3 ΔN_2O/AOU relationship

A two-linear ΔN_2O/AOU relationship has been identified in the upper oxycline for waters with oxygen concentrations higher than 50 µM and between 50 µM and 5 µM during the M77-4 cruise that took place in the offshore waters of the OMZ (Ryabenko et al., 2012). We found a very similar relationship for all offshore data with oxygen concentrations above 50 µM with no systematic difference between the data from the M77-4 (January/February 2009) cruise and the M90 (November 2012) cruise (Figures 2, 6a). This indicates a comparable setting of the open ocean OMZ waters during both cruises. We furthermore found no difference in the ΔN_2O/AOU relationship between stations with a broad N_2O maximum and a double-peak structure. These results are similar to previously reported ΔN_2O/AOU relationships from other oceanic OMZs (Upstill-Goddard et al., 1999; Cohen and Gordon, 1978; De Wilde and Helder, 1997).

In contrast to the open ocean waters, a correlation between ΔN_2O and AOU was not observed for the coastal data (Fig. 6b). Numerous values with much higher ΔN_2O/AOU ratios than in the offshore waters were observed. These data were highly scattered over the full range of oxygen concentrations. The ΔN_2O values that showed the strongest deviation from the offshore ΔN_2O/AOU ratio were associated with highly negative N’ values as a signal for a large nitrogen deficit (Fig. 6b). This indicates that these waters with extreme N_2O accumulation had been subject to extensive N loss.

4 Discussion

To understand the differences between the offshore and the coastal N_2O distribution in the Peruvian upwelling, the factors that influence N_2O production or consumption during nitrification and denitrification need to be investigated.

In the oxycline waters of OMZs, peak N_2O production from nitrification as well as denitrification has been determined under suboxic conditions, whereas N_2O depletion was dominant in the OMZ core (Ji et al., 2015). Rate measurements however provided evidence that N_2O production and consumption co-occur and that interplay between N_2O production and consumption processes regulates net N_2O accumulation or depletion in the water column (Babbin et al., 2015). In open ocean OMZs, however, N_2O profiles reveal a remarkably stable shape which indicates that in these areas N_2O production and consumption processes are well balanced (Babbin et al., 2015). Except for differences between the offshore N_2O profiles with a broad N_2O maximum north of 5 °S and a double-peak structure south of 5°S, the offshore N_2O profiles observed in our study indeed showed a relatively invariant N_2O distribution. The differences in the shape of the N_2O profiles can be explained by changing oxygen concentrations in the OMZ core and a threshold oxygen concentration of 5 µM for net N_2O consumption.

In areas where highly oxygen-deficient waters extended over the continental shelf, extreme accumulation of N_2O has been found before in the Arabian Sea (Naqvi et al., 2010; Naqvi et al., 2006) and off Chile (Farías et al., 2015) and has been explained by rapid changes in the environmental conditions: Naqvi et al. (2000) explained the extreme N_2O accumulation over the Indian shelf with the response of denitrifying enzymes to transient oxygen depletion. N_2O thus accumulated when waters reached suboxic conditions. N_2O accumulation coincided with the accumulation of nitrite and consumption of N_2O started when these waters became sulfidic (Naqvi et al., 2010). Farías et al. (2015) measured N_2O accumulation during the transition from oxic to anoxic conditions, too, but at variable oxygen concentrations whereas N_2O depletion became dominant under suboxic conditions.

In contrast to the results from the Indian Ocean, they identified enhanced remineralization due to short-term variability in coastal upwelling as the main driver for N_2O accumulation.

The large variability we observed in the N_2O distribution at the Peruvian coast could also be explained by an imbalance between N_2O production and consumption processes that may lead to its accumulation. This could have been induced by rapid changes of the oxygen concentrations in the coastal upwelling zone: enhanced mixing of oxygen-rich and oxygen deficient waters and exchange of upwelled waters with the atmosphere supply oxygen to the water column (Schafstall et al., 2010; Thomsen et al., 2016 ; Pietri et al., 2014) while strong remineralization leads to rapid oxygen consumption (Kalvelage et al., 2015). Kalvelage et al. (2011) furthermore showed that these high remineralization rates also induce strong N cycling in the subsurface layer. Turnover rates for different N species are therefore much faster on the shelf than in the open ocean OMZ (Hu et al., 2015), which is also reflected in the distribution of different functional gene abundances (Löscher et al., 2014). Hence, it is likely that N_2O production and consumption rates are much higher at the coast than in the offshore waters, and that short periods of increased N_2O production could lead to very high N_2O accumulation.

Changes in the oxygen concentrations could influence N_2O production from nitrification as well as from denitrification: enhanced production of N_2O after transition from anoxic to oxic conditions is a known process occurring in soils (e.g. Morley et al., 2008) and may be explained by a different sensitivity of denitrifying enzymes to trace concentrations of oxygen (Tiedje, 1988). In a recent incubation study, Dalsgaard et al. (2014) found no indication of increased N_2O production by denitrification due to changes in the oxygen concentration at nanomolar levels, however. Instead, autotrophic denitrification and N_2O production have been shown to be stimulated by the addition of hydrogen sulfide (H_2S) (Galan et al., 2014; Dalsgaard et al., 2014). We did not find direct evidence for a coupling between N_2O production and the presence of H_2S in our measurements, as high N_2O accumulation was often found in proximity to H_2S plumes but was also detected when H_2S was absent in the water column. We cannot exclude that the high N_2O production we frequently observed at the shelf was stimulated by a coupling of denitrification with sulfur cycling, though: Canfield et al. (2010) found evidence for active sulfur cycling in the ETSP without H_2S accumulation, and a coupling between H_2S oxidation and denitrification has been shown before (Galan et al., 2014; Jensen et al., 2009). Indeed, active denitrification was found in proximity to H_2S plumes in the water column during M77-3 (Kalvelage et al., 2013; Schunck et al., 2013).

In the ocean, increased N_2O production was also associated with the onset of nitrification after re-ventilation of the water column in a seasonal study in the Baltic Sea, but with relatively low resulting N_2O concentrations (Naqvi et al., 2010). Yu et al. (2010) found strongly increased N_2O production by nitrifying bacteria that was stimulated by the availability of ammonium during recovery from anoxic conditions in a chemostat culture experiment. Their results point towards an increased N_2O production via the ammonium-oxidation pathway, while N_2O production by nitrifier-denitrification seemed not to be stimulated by the shift from anoxic to oxic conditions. We frequently measured high ammonium concentrations along the Peruvian shelf, indeed (Fig. 4), which could have stimulated N_2O production from ammonium oxidation. A direct correlation between N_2O and ammonium could not be identified, however.

From our concentration measurements alone we thus cannot distinguish if the observed high production of N_2O is a result of denitrification or nitrification processes. Studies of the isotopic and isotopomeric N_2O composition and N_2O production and consumption rate measurements could reveal more detailed insights whether N_2O is produced via the ammonium oxidation or the nitrite reduction pathway during its extreme accumulation.

In our study, we found strongly elevated N_2O concentrations (>100 nM) over the full range of oxygen concentrations, coinciding with strong N depletion (Fig. 5), but without nitrite accumulation (Fig. 4). The high oxygen concentrations found in the majority of our samples with extreme N_2O accumulation and N depletion excludes in-situ denitrification or anammox (see e.g. Babbin et al., 2014; Dalsgaard et al., 2014).

The extraordinarily high N_2O concentrations as well as the low N' values thus have to be old signals of processes taking place under anoxic to suboxic conditions. There is no known consumption process for N_2O in oxygenated waters (Bange, 2008), and the strong signals of N loss that are produced under anoxic conditions are unlikely to be rapidly compensated by N fixation upon oxygenation. Both signals thus are likely to have remained preserved when oxygen concentrations increased due to mixing with waters of higher oxygen concentration or due to direct contact with the atmosphere as a result of upwelling.

Our observations of high N_2O concentrations in oxygenated waters furthermore indicate that this accumulation could have taken place during re-oxygenation rather than during decreasing oxygen concentrations. An increase in oxygen concentrations would lead to the preservation of the high N_2O signals in the water column whereas further decreasing oxygen concentrations would only lead to a temporal N_2O accumulation and would eventually stimulate N_2O consumption.

5 Summary and Conclusions

We observed extreme N_2O accumulations over the Peruvian shelf and in the adjacent waters with maximum concentrations similar to the observations by Naqvi et al. (2000) over the West Indian shelf and Farías et al. (2015) off Chile, whereas N_2O concentrations in the open ocean OMZ off Peru were comparably moderate. Similar to the findings by Naqvi et al. (2000), we found that N_2O accumulation could be caused by enhanced N_2O production by nitrification or denitrification under transient oxygen concentrations. We found strong evidence that these N_2O accumulations are preserved when oxygen concentrations increased as a result of mixing and exchange with the overlying atmosphere in the upwelling zone. Waters with high N_2O concentrations can thus be directly and frequently transported to the surface ocean. This makes this region one of the most important oceanic regions for N_2O emissions to the atmosphere (Arévalo-Martínez et al., 2015). This direct link between unusually high N_2O production and emissions over the Peruvian shelf makes it necessary to understand the biogeochemical processes involved in N_2O production and consumption to produce reliable predictions of oceanic emissions from this area. Current approaches to model the N_2O distribution rely on parameterizations based on the linear ΔN_2O/AOU relationship (Suntharalingam and Sarmiento, 2000; Nevison et al., 2003; Freing et al., 2012). These approaches could in fact reproduce the oxygen distribution in the open ocean OMZ off Peru reasonably well, but they fail to account for the extreme N_2O accumulation and its high spatial and temporal variability over the shelf area. They thus significantly underestimate the emissions from the Peruvian upwelling and potentially other upwelling areas with similar conditions, too.

Author Contribution

A. Kock, D. Arévalo-Martínez, H. Bange and C. Löscher designed the sampling strategy and conducted the N_2O sampling and measurements. A. Kock and C. Löscher analyzed the N_2O measurement data and calculated in-situ N_2O concentrations. A. Kock conducted the further data analysis and wrote the paper with contributions from all co-authors.

Acknowledgements

We would like to thank the captains and crew of the R/V Meteor for their professional support and the chief scientists of M77-3 & M90-M93, Martin Frank, Lothar Stramma, Stefan Sommer and Gaute Lavik for the opportunity to collect samples during their cruises. We would also like to thank Annie Bourbonnais and Johanna Maltby for the collection of N_2O samples during M92, and Gesa Eirund, Joel Craig, Georgina Flores, Jennifer Zur, Moritz Baumann, Tina Baustian and Dörte Nitschkowski for their help in analyzing the samples.

We would like to thank Frank Malien, Mirja Dunker, Violeta Leon, Peter Fritsche, Tina Baustian, Kerstin Nachtigall, Martina Lohmann, Gabriele Klockgether and Tim Kalvelage for the sampling and analysis of oxygen and nutrient samples during M77-3 & M77-4 and M90-M93. The work presented here was made possible by the DFG-supported projects SFB754 Phase I and II (http://www.sfb754.de) and the BMBF joint projects SOPRAN II and III (FKZ 03F0611A and FKZ 03F662A).

References

Altabet, M. A., Ryabenko, E., Stramma, L., Wallace, D. W. R., Frank, M., Grasse, P., and Lavik, G.: An eddy-stimulated hotspot for fixed nitrogen-loss from the Peru oxygen minimum zone, Biogeosciences, 9, 4897-4908, 10.5194/bg-9-4897-2012, 2012.

Arévalo-Martínez, D. L., Beyer, M., Krumbholz, M., Piller, I., Kock, A., Steinhoff, T., Kortzinger, A., and Bange, H. W.: A new method for continuous measurements of oceanic and atmospheric N2O, CO and CO2: performance of off-axis integrated cavity output spectroscopy (OA-ICOS) coupled to non-dispersive infrared detection (NDIR), Ocean Science, 9, 1071-1087, 10.5194/os-9-1071-2013, 2013.

Arévalo-Martínez, D. L., Kock, A., Löscher, C. R., Schmitz, R. A., and Bange, H. W.: Massive nitrous oxide emissions from the tropical South Pacific Ocean, Nature Geosci, 8, 530-533, 10.1038/ngeo2469 http://www.nature.com/ngeo/journal/vaop/ncurrent/abs/ngeo2469.html#supplementary-information, 2015.

Arp, D. J., and Stein, L. Y.: Metabolism of inorganic N compounds by ammonia-oxidizing bacteria, Critical Reviews in Biochemistry and Molecular Biology, 38, 471-495, 10.1080/10409230390267446, 2003.

Babbin, A. R., Keil, R. G., Devol, A. H., and Ward, B. B.: Organic Matter Stoichiometry, Flux, and Oxygen Control Nitrogen Loss in the Ocean, Science, 344, 406-408, 10.1126/science.1248364, 2014.

Babbin, A. R., Bianchi, D., Jayakumar, A., and Ward, B. B.: Rapid nitrous oxide cycling in the suboxic ocean, Science, 348, 1127-1129, 10.1126/science.aaa8380, 2015.

Bange, H. W., Andreae, M. O., Lal, S., Law, C. S., Naqvi, S. W. A., Patra, P. K., Rixen, T., and Upstill-Goddard, R. C.: Nitrous oxide emissions from the Arabian Sea: A synthesis, Atmospheric Chemistry and Physics, 1, 61-71, 2001.

Bange, H. W.: Gaseous nitrogen compounds (NO,N2O,N2,NH3) in the ocean, in: Nitrogen in the Marine Environment, 2 ed., edited by: Capone, D. G., Bronk, D. A., Mulholland, M. R., and Carpenter, E. J., Academic Press/Elsevier 51-94, 2008.

Canfield, D. E., Stewart, F. J., Thamdrup, B., De Brabandere, L., Dalsgaard, T., Delong, E. F., Revsbech, N. P., and Ulloa, O.: A Cryptic Sulfur Cycle in Oxygen-Minimum-Zone Waters off the Chilean Coast, Science, 330, 1375-1378, 10.1126/science.1196889, 2010.

Chaigneau, A., Dominguez, N., Eldin, G., Vasquez, L., Flores, R., Grados, C., and Echevin, V.: Near-coastal circulation in the Northern Humboldt Current System from shipboard ADCP data, Journal of Geophysical Research-Oceans, 118, 5251-5266, 10.1002/jgrc.20328, 2013.

Chang, B. X., Rich, J. R., Jayakumar, A., Naik, H., Pratihary, A. K., Keil, R. G., Ward, B. B., and Devol, A. H.: The effect of organic carbon on fixed nitrogen loss in the eastern tropical South Pacific and

Arabian Sea oxygen deficient zones, Limnology and Oceanography, 59, 1267-1274, 10.4319/lo.2014.59.4.1267, 2014.

Charpentier, J., Farias, L., and Pizarro, O.: Nitrous oxide fluxes in the central and eastern South Pacific, Global Biogeochemical Cycles, 24, -, Artn Gb3011 Doi 10.1029/2008gb003388, 2010.

Chavez, F. P., and Messié, M.: A comparison of Eastern Boundary Upwelling Ecosystems, Prog. Oceanogr., 83, 80-96, 2009.

Chelton, D. B., DeSzoeke, R. A., Schlax, M. G., El Naggar, K., and Siwertz, N.: Geographical variability of the first baroclinic Rossby radius of deformation, Journal of Physical Oceanography, 28, 433-460, 10.1175/1520-0485(1998)028<0433:gvotfb>2.0.co;2, 1998.

Ciais, P., Sabine, C. L., Bala, G., Bopp, L., Brovkin, V., Canadell, J., Chhabra, A., DeFries, R., Galloway, J. N., Heimann, M., Jones, C., Le Quéré, C., Myneni, R., Piao, S., and Thornton, P.: Carbon and other Biogeochemical Cycles, in: Climate Change 2013: The Physical Science Basis. Contribution of Working Group I to the Fifth Assessment Report of the Intergovernmental Panel on Climate Change, edited by: Stocker, T. F., Qin, D., Plattner, G.-K., Tignor, M., Allen, S. K., Boschung, J., Nauels, A., Xia, Y., Bex, V., and Midgley, P. M., Cambridge University Press, Cambridge, UK, and New York, NY, USA, 465-570, 2013.

Codispoti, L. A., and Christensen, J. P.: Nitrification, denitrification and nitrous oxide cycling in the eastern tropical South Pacific Ocean, Marine Chemistry, 16, 277-300, 1985.

Codispoti, L. A., Friederich, G. E., Packard, T. T., Glover, H. E., Kelly, P. J., Spinrad, R. W., Barber, R. T., Elkins, J. W., Ward, B. B., Lipschultz, F., and Lostaunau, N.: High nitrite levels off northern Peru: A signal of instability in the marine denitrification rate, Science, 233, 1200-1202, 1986.

Cohen, Y., and Gordon, L. I.: Nitrous oxide in oxygen minimum of eastern tropical North Pacific - evidence for its consumption during denitrification and possible mechanisms for its production, Deep-Sea Research, 25, 509-524, 10.1016/0146-6291(78)90640-9, 1978.

Cornejo, M., and Farias, L.: Following the N2O consumption in the oxygen minimum zone of the eastern South Pacific, Biogeosciences, 9, 3205-3212, 10.5194/bg-9-3205-2012, 2012.

Dalsgaard, T., Stewart, F. J., Thamdrup, B., De Brabandere, L., Revsbech, N. P., Ulloa, O., Canfield, D. E., and DeLong, E. F.: Oxygen at Nanomolar Levels Reversibly Suppresses Process Rates and Gene Expression in Anammox and Denitrification in the Oxygen Minimum Zone off Northern Chile, Mbio, 5, UNSP e01966 10.1128/mBio.01966-14, 2014.

De Wilde, H. P. J., and Helder, W.: Nitrous oxide in the Somali Basin: the role of upwelling, Deep Sea Research Part II: Topical Studies in Oceanography, 44, 1319-1340, http://dx.doi.org/10.1016/S0967-0645(97)00011-8, 1997.

Dewitte, B., Vazquez-Cuervo, J., Goubanova, K., Illig, S., Takahashi, K., Cambon, G., Purca, S., Correa, D., Gutierrez, D., Sifeddine, A., and Ortlieb, L.: Change in El Nino flavours over 1958-2008: Implications for the long-term trend of the upwelling off Peru, Deep-Sea Res Pt Ii, 77-80, 143-156, 10.1016/j.dsr2.2012.04.011, 2012.

Echevin, V., Aumont, O., Ledesma, J., and Flores, G.: The seasonal cycle of surface chlorophyll in the Peruvian upwelling system: A modelling study, Prog. Oceanogr., 79, 167-176, http://dx.doi.org/10.1016/j.pocean.2008.10.026, 2008.

Farias, L., Paulmier, A., and Gallegos, M.: Nitrous oxide and N-nutrient cycling in the oxygen minimum zone off northern Chile, Deep-Sea Research Part I-Oceanographic Research Papers, 54, 164-180, 10.1016/j.dsr.2006.11.003, 2007.

Farias, L., Castro-Gonzalez, M., Cornejo, M., Charpentier, J., Faundez, J., Boontanon, N., and Yoshida, N.: Denitrification and nitrous oxide cycling within the upper oxycline of the eastern tropical South Pacific oxygen minimum zone, Limnology and Oceanography, 54, 132-144, 2009.

Farías, L., Besoain, V., and García-Loyola, S.: Presence of nitrous oxide hotspots in the coastal upwelling area off central Chile: an analysis of temporal variability based on ten years of a biogeochemical time series, Environmental Research Letters, 10, 044017, 10.1088/1748-9326/10/4/04, 2015.

Firestone, M. K., Firestone, R. B., and Tiedje, J. M.: Nitrous-oxide from soil denitrification - factors controlling its biological production, Science, 208, 749-751, 10.1126/science.208.4445.749, 1980.

Forster, G., Upstill-Goddard, R. C., Gist, N., Robinson, C., Uher, G., and Woodward, E. M. S.: Nitrous oxide and methane in the Atlantic Ocean between 50 degrees N and 52 degrees S: Latitudinal distribution and sea-to-air flux, Deep-Sea Res Pt Ii, 56, 964-976, 10.1016/j.dsr2.2008.12.002, 2009.

Freing, A., Wallace, D. W. R., Tanhua, T., Walter, S., and Bange, H. W.: North Atlantic production of nitrous oxide in the context of changing atmospheric levels, Global Biogeochem. Cycles, 23, 10.1029/2009gb003472, 2009.

Freing, A., Wallace, D. W. R., and Bange, H. W.: Global oceanic production of nitrous oxide, Philosophical Transactions of the Royal Society B-Biological Sciences, 367, 1245-1255, 10.1098/rstb.2011.0360, 2012.

Fuenzalida, R., Schneider, W., Garcés-Vargas, J., Bravo, L., and Lange, C.: Vertical and horizontal extension of the oxygen minimum zone in the eastern South Pacific Ocean, Deep Sea Research Part II: Topical Studies in Oceanography, 56, 992-1003, 2009.

Galan, A., Faundez, J., Thamdrup, B., Francisco Santibanez, J., and Farias, L.: Temporal dynamics of nitrogen loss in the coastal upwelling ecosystem off central Chile: Evidence of autotrophic denitrification through sulfide oxidation, Limnology and Oceanography, 59, 1865-1878, 10.4319/lo.2014.59.6.1865, 2014.

Goreau, T. J., Kaplan, W. A., Wofsy, S. C., McElroy, M. B., Valois, F. W., and Watson, S. W.: Production of NO_2^- and N_2O by nitrifying bacteria at reduced concentrations of oxygen, Appl. Environ. Microbiol., 40, 526-532, 1980.

Graco, M., Purca, S., Dewitte, B., Morón, O., Ledesma, J., Flores, G., Castro, C., and Gutiérrez, D.: The OMZ and nutrients features as a signature of interannual and low frequency variability off the peruvian upwelling system, Biogeosciences Discuss., 2016, 1-36, 10.5194/bg-2015-567, 2016.

Gutierrez, D., Enriquez, E., Purca, S., Quipuzcoa, L., Marquina, R., Flores, G., and Graco, M.: Oxygenation episodes on the continental shelf of central Peru: Remote forcing and benthic ecosystem response, Prog. Oceanogr., 79, 177-189, 10.1016/j.pocean.2008.10.025, 2008.

Hamersley, M. R., Lavik, G., Woebken, D., Rattray, J. E., Lam, P., Hopmans, E. C., Sinninghe Damste, J. S., Krueger, S., Graco, M., Gutierrez, D., and Kuypers, M. M. M.: Anaerobic ammonium oxidation in the Peruvian oxygen minimum zone, Limnology and Oceanography, 52, 923-933, 2007.

Hansen, H. P., and Koroleff, F.: Determination of nutrients, in: Methods of seawater analysis, edited by: Grasshoff, K., Kremling, K., and Ehrhardt, M., Wiley-VCH, Weinheim, 159-228, 1999.

Hu, H., Bourbonnais, A., Larkum, J., Bange, H. W., and Altabet, M. A.: Nitrogen cycling in shallow low oxygen coastal waters off Peru from nitrite and nitrate nitrogen and oxygen isotopes, Biogeosciences Discuss., 12, 7257-7299, 10.5194/bgd-12-7257-2015, 2015.

IPCC: Climate Change 2013: The Physical Science Basis. Contribution of Working Group I to the Fifth Assessment Report of the Intergovernmental Panel on Climate Change., Cambridge, UK and New York, NY, 1535, 2013.

Jensen, M. M., Petersen, J., Dalsgaard, T., and Thamdrup, B.: Pathways, rates, and regulation of N-2 production in the chemocline of an anoxic basin, Mariager Fjord, Denmark, Marine Chemistry, 113, 102-113, 10.1016/j.marchem.2009.01.002, 2009.

Ji, Q., Babbin, A. R., Jayakumar, A., Oleynik, S., and Ward, B. B.: Nitrous oxide production by nitrification and denitrification in the Eastern Tropical South Pacific oxygen minimum zone, Geophysical Research Letters, 42, 2015GL066853, 10.1002/2015gl066853, 2015.

Kalvelage, T., Jensen, M. M., Contreras, S., Revsbech, N. P., Lam, P., Guenter, M., LaRoche, J., Lavik, G., and Kuypers, M. M. M.: Oxygen Sensitivity of Anammox and Coupled N-Cycle Processes in Oxygen Minimum Zones, Plos One, 6, e29299
10.1371/journal.pone.0029299, 2011.

Kalvelage, T., Lavik, G., Lam, P., Contreras, S., Arteaga, L., Loescher, C. R., Oschlies, A., Paulmier, A., Stramma, L., and Kuypers, M. M. M.: Nitrogen cycling driven by organic matter export in the South Pacific oxygen minimum zone, Nature Geoscience, 6, 228-234, 10.1038/ngeo1739, 2013.

Kalvelage, T., Lavik, G., Jensen, M. M., Revsbech, N. P., Loescher, C., Schunck, H., Desai, D. K., Hauss, H., Kiko, R., Holtappels, M., LaRoche, J., Schmitz, R. A., Graco, M. I., and Kuypers, M. M. M.: Aerobic Microbial Respiration In Oceanic Oxygen Minimum Zones, Plos One, 10, e0133526 10.1371/journal.pone.0133526, 2015.

Karstensen, J., Stramma, L., and Visbeck, M.: Oxygen minimum zones in the eastern tropical Atlantic and Pacific oceans, Prog. Oceanogr., 77, 331-350, 10.1016/j.pocean.2007.05.009, 2008.

Kock, A., and Bange, H. W.: Counting the ocean's greenhouse gas emissions, Eos, 96, 10-13, 10.1029/2015EO023665, 2015.

Law, C. S., and Owens, N. J. P.: Significant flux of atmospheric nitrous oxide from the Northwest Indian Ocean, Nature, 346, 826-828, 10.1038/346826a0, 1990.

Löscher, C. R., Kock, A., Könneke, M., LaRoche, J., Bange, H. W., and Schmitz, R. A.: Production of oceanic nitrous oxide by ammonia-oxidizing archaea, Biogeosciences, 9, 2419-2429, 10.5194/bg-9-2419-2012, 2012.

Löscher, C. R., Grosskopf, T., Desai, F. D., Gill, D., Schunck, H., Croot, P. L., Schlosser, C., Neulinger, S. C., Pinnow, N., Lavik, G., Kuypers, M. M. M., LaRoche, J., and Schmitz, R. A.: Facets of diazotrophy in the oxygen minimum zone waters off Peru, Isme Journal, 8, 2180-2192, 10.1038/ismej.2014.71, 2014.

Messie, M., Ledesma, J., Kolber, D. D., Michisaki, R. P., Foley, D. G., and Chavez, F. P.: Potential new production estimates in four eastern boundary upwelling ecosystems, Prog. Oceanogr., 83, 151-158, 10.1016/j.pocean.2009.07.018, 2009.

Montes, I., Colas, F., Capet, X., and Schneider, W.: On the pathways of the equatorial subsurface currents in the eastern equatorial Pacific and their contributions to the Peru-Chile Undercurrent, Journal of Geophysical Research-Oceans, 115, C09003 10.1029/2009jc005710, 2010.

Morley, N., Baggs, E. M., Dorsch, P., and Bakken, L.: Production of NO, N(2)O and N(2) by extracted soil bacteria, regulation by NO(2)(-) and O(2) concentrations, FEMS Microbiol. Ecol., 65, 102-112, 10.1111/j.1574-6941.2008.00495.x, 2008.

Naqvi, S. W. A., Jayakumar, D. A., Narveka, P. V., Naik, H., Sarma, V. V. S. S., D'Souza, W., Joseph, S., and George, M. D.: Increased marine production of N_2O due to intensifying anoxia on the Indian continental shelf, Nature, 408, 346-349, 2000.

Naqvi, S. W. A., Naik, H., Pratihary, A., D'Souza, W., Narvekar, P. V., Jayakumar, D. A., Devol, A. H., Yoshinari, T., and Saino, T.: Coastal versus open-ocean denitrification in the Arabian Sea, Biogeosciences, 3, 621-633, 2006.

Naqvi, S. W. A., Bange, H. W., Farias, L., Monteiro, P. M. S., Scranton, M. I., and Zhang, J.: Marine hypoxia/anoxia as a source of CH4 and N2O, Biogeosciences, 7, 2159-2190, 10.5194/bg-7-2159-2010, 2010.

Nevison, C., Butler, J. H., and Elkins, J. W.: Global distribution of N2O and the Delta N2O-AOU yield in the subsurface ocean, Global Biogeochemical Cycles, 17, 1119 10.1029/2003gb002068, 2003.

Nevison, C. D., Lueker, T. J., and Weiss, R. F.: Quantifying the nitrous oxide source from coastal upwelling, Global Biogeochem. Cycles, 18, GB1018 10.1029/2003GB002110, 2004.

Ni, B.-J., Peng, L., Law, Y., Guo, J., and Yuan, Z.: Modeling of Nitrous Oxide Production by Autotrophic Ammonia-Oxidizing Bacteria with Multiple Production Pathways, Environmental Science & Technology, 48, 3916-3924, 10.1021/es405592h, 2014.

Ostrom, N. E., Russ, M. E., Popp, B., Rust, T. M., and Karl, D. M.: Mechanisms of nitrous oxide production in the subtropical North Pacific based on determinations of the isotopic abundances of nitrous oxide and di-oxygen, Chemosphere - Global Change Science, 2, 281-290, 2000.

Paulmier, A., Ruiz-Pino, D., Garcon, V., and Farias, L.: Maintaining of the Eastern South Pacific Oxygen Minimum Zone (OMZ) off Chile, Geophysical Research Letters, 33, L20601 10.1029/2006gl026801, 2006.

Pennington, J. T., Mahoney, K. L., Kuwahara, V. S., Kolber, D. D., Calienes, R., and Chavez, F. P.: Primary production in the eastern tropical Pacific: A review, Prog. Oceanogr., 69, 285-317, 10.1016/j.pocean.2006.03.012, 2006.

Pietri, A., Testor, P., Echevin, V., Chaigneau, A., Mortier, L., Eldin, G., and Grados, C.: Finescale Vertical Structure of the Upwelling System off Southern Peru as Observed from Glider Data, Journal of Physical Oceanography, 43, 631-646, 10.1175/jpo-d-12-035.1, 2013.

Pietri, A., Echevin, V., Testor, P., Chaigneau, A., Mortier, L., Grados, C., and Albert, A.: Impact of a coastal-trapped wave on the near-coastal circulation of the Peru upwelling system from glider data, Journal of Geophysical Research-Oceans, 119, 2109-2120, 10.1002/2013jc009270, 2014.

Ryabenko, E., Kock, A., Bange, H. W., Altabet, M. A., and Wallace, D. W. R.: Contrasting biogeochemistry of nitrogen in the Atlantic and Pacific Oxygen Minimum Zones, Biogeosciences, 9, 203-215, 10.5194/bg-9-203-2012, 2012.

Santoro, A. E., Buchwald, C., McIlvin, M. R., and Casciotti, K. L.: Isotopic Signature of N(2)O Produced by Marine Ammonia-Oxidizing Archaea, Science, 333, 1282-1285, 10.1126/science.1208239, 2011.

Schneider, W., Fuenzalida, R., Rodriguez-Rubio, E., Garces-Vargas, J., and Bravo, L.: Characteristics and formation of eastern South Pacific intermediate water, Geophysical Research Letters, 30, 1581 10.1029/2003gl017086, 2003.

Schunck, H., Lavik, G., Desai, D. K., Grosskopf, T., Kalvelage, T., Loescher, C. R., Paulmier, A., Contreras, S., Siegel, H., Holtappels, M., Rosenstiel, P., Schilhabel, M. B., Graco, M., Schmitz, R. A., Kuypers, M. M. M., and LaRoche, J.: Giant Hydrogen Sulfide Plume in the Oxygen Minimum Zone off Peru Supports Chemolithoautotrophy, Plos One, 8, e68661 10.1371/journal.pone.0068661, 2013.

Stein, L. Y.: Surveying N_2O-producing pathways in bacteria, in: Methods in Enzymology: Research on Nitrification and Related Processes, Vol 486, Part A, edited by: Klotz, M. G., Methods in Enzymology, 131-152, 2011.

Stieglmeier, M., Mooshammer, M., Kitzler, B., Wanek, W., Zechmeister-Boltenstern, S., Richter, A., and Schleper, C.: Aerobic nitrous oxide production through N-nitrosating hybrid formation in ammonia-oxidizing archaea, Isme Journal, 8, 1135-1146, 10.1038/ismej.2013.220, 2014.

Stramma, L., Johnson, G. C., Firing, E., and Schmidtko, S.: Eastern Pacific oxygen minimum zones: Supply paths and multidecadal changes, Journal of Geophysical Research-Oceans, 115, C09011 10.1029/2009jc005976, 2010.

Suntharalingam, P., and Sarmiento, J. L.: Factors governing the oceanic nitrous oxide distribution: Simulations with an ocean general circulation model, Global Biogeochemical Cycles, 14, 429-454, 10.1029/1999gb900032, 2000.

Thamdrup, B., Dalsgaard, T., Jensen, M. M., Ulloa, O., Farias, L., and Escribano, R.: Anaerobic ammonium oxidation in the oxygen-deficient waters off northern Chile, Limnology and Oceanography, 51, 2145-2156, 2006.

Thamdrup, B., Dalsgaard, T., and Revsbech, N. P.: Widespread functional anoxia in the oxygen minimum zone of the Eastern South Pacific, Deep-Sea Research Part I-Oceanographic Research Papers, 65, 36-45, 10.1016/j.dsr.2012.03.001, 2012.

Thomsen, S., Kanzow, T., Krahmann, G., Greatbatch, R. J., Dengler, M., and Lavik, G.: The formation of a subsurface anticyclonic eddy in the Peru-Chile Undercurrent and its impact on the near-coastal salinity, oxygen, and nutrient distributions, Journal of Geophysical Research: Oceans, n/a-n/a, 10.1002/2015jc010878, 2016.

Tiedje, J. M.: Ecology of denitrification and dissimilatory nitrate reduction to ammonium, in: Biology of anearobic microorganisms, edited by: Zehnder, A. J. B., Wiley & Sons, New York, 179-244, 1988.

Upstill-Goddard, R. C., Barnes, J., and Owens, N. J. P.: Nitrous oxide and methane during the 1994 SW monsoon in the Arabian Sea/northwestern Indian Ocean, Journal of Geophysical Research-Oceans, 104, 30067-30084, 10.1029/1999jc900232, 1999.

Walker, C. B., de la Torre, J. R., Klotz, M. G., Urakawa, H., Pinel, N., Arp, D. J., Brochier-Armanet, C., Chain, P. S. G., Chan, P. P., Gollabgir, A., Hemp, J., Hugler, M., Karr, E. A., Konneke, M., Shin, M., Lawton, T. J., Lowe, T., Martens-Habbena, W., Sayavedra-Soto, L. A., Lang, D., Sievert, S. M., Rosenzweig, A. C., Manning, G., and Stahl, D. A.: Nitrosopumilus maritimus genome reveals unique mechanisms for nitrification and autotrophy in globally distributed marine crenarchaea, Proceedings of the National Academy of Sciences of the United States of America, 107, 8818-8823, 10.1073/pnas.0913533107, 2010.

Walter, S., Bange, H. W., Breitenbach, U., and Wallace, D. W. R.: Nitrous oxide in the North Atlantic Ocean, Biogeosciences, 3, 607-619, 10.5194/bg-3-607-2006, 2006.

Weiss, R. F., and Price, B. A.: Nitrous oxide solubility in water and seawater, Mar. Chem., 8, 347-359, 1980.

WMO: Scientific Assessment of Ozone Depletion: 2010, Global Ozone Research and Monitoring Project, Geneva, Switzerland, 2011.

Wyrtki, K.: CIRCULATION AND WATER MASSES IN EASTERN EQUATORIAL PACIFIC OCEAN, International Journal of Oceanology and Limnology, 1, 117-&, 1967.

Yu, R., Kampschreur, M. J., Loosdrecht, M. C. M. v., and Chandran, K.: Mechanisms and Specific Directionality of Autotrophic Nitrous Oxide and Nitric Oxide Generation during Transient Anoxia, Environmental Science & Technology, 44, 1313-1319, 10.1021/es902794a, 2010.

Zamora, L. M., Oschlies, A., Bange, H. W., Huebert, K. B., Craig, J. D., Kock, A., and Loscher, C. R.: Nitrous oxide dynamics in low oxygen regions of the Pacific: insights from the MEMENTO database, Biogeosciences, 9, 5007-5022, 10.5194/bg-9-5007-2012, 2012.

Figures:

Figure 1: Station maps of the sampled N_2O stations from cruises A) M77-3, December 2008 – January 2009 (●) and M77-4, January – February 2009 (⊙), B) M90, November 2012 (●) and M91, December 2012 (⊙), C) M92, January 2013 (●) and M93, February – March 2013 (⊙). Section annotations in A) and B) correspond to the vertical sections shown in Fig. 2 and 3.

Figure 2: Spatial distributions of oxygen (A, B), nitrite (C, D) and N_2O (E, F) along 86°W during M77-4 (2009, A, C, E) and M90 (2012, B, D, F). Small dots indicate location and depth of the discrete samples. Data gridding: ODV/DIVA.

Figure 3: Cross-shelf distribution of A) Oxygen, B) Phosphate, C) Nitrate, D) N', e) Nitrite and f) N_2O during M91 (Section F).

Figure 4: Selected depth profiles of oxygen (black dots, dotted line), potential density (σ_θ, grey line) and N_2O (red line, open circles) (left panel) and nitrate (grey line), nitrite (black circles, dotted line), ammonium (blue diamonds, straight line) and N' (red line, small dots) (right panel) from selected open ocean and shelf stations during M90-93. Depth profiles of oxygen and σ_θ were taken from the CTD sensors, whereas the other parameters were taken from discrete samples. The locations of the respective stations are shown in the map. Red signals denote stations classified as "coastal" stations whereas blue signals denote "offshore" stations. Please note the changes in the scales for N_2O, σ_θ, nitrite and ammonium.

Figure 5: Temperature-Salinity diagrams with ΔN_2O color coded for a) the offshore stations and b) the onshore stations. Gray symbols denote the T-S properties of a) the onshore and b) the offshore data. The approximate location of the different water masses annotated in the figure is given by black dots or lines. Different symbols denote different cruises: □ M77-3; ◊ M77-4; ○ M92; ▷M90; ◁ M91; ✻M93.

Figure 6: ΔN_2O/AOU relationship from a) offshore stations and b) coastal stations. Samples from the upper OMZ and oxycline (sample depth < 350 m) are color coded with N', whereas samples from below 350 m are shown in gray. Different symbols for different cruises are denoted the same as in Figure 5. The black line denotes the ΔN_2O/AOU relationship from the offshore data for samples with O_2>50 µM and depth < 350 m (y=0.13x+3.73; r^2=0.83). Please note the change in the scaling for ΔN_2O values of 0 - 100 nM and 100 - 1000 nM (dotted line).

Figure 1:

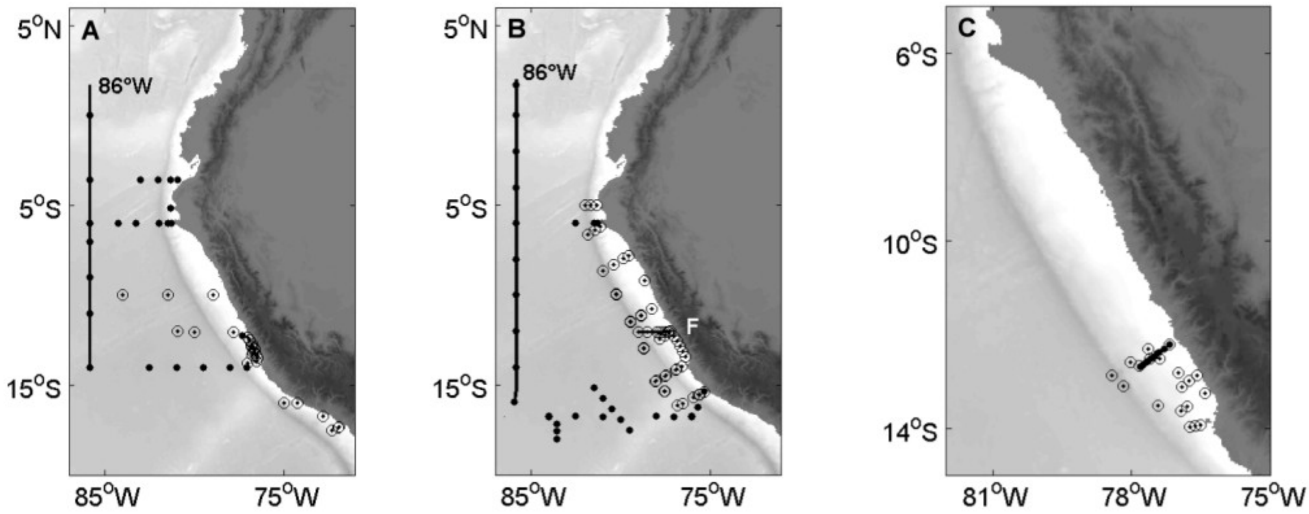
A
86°W
5°N
5°S
15°S
85°W
75°W
B
86°W
F
5°N
5°S
15°S
85°W
75°W
C
6°S
10°S
14°S
81°W
78°W
75°W

Figure 2:

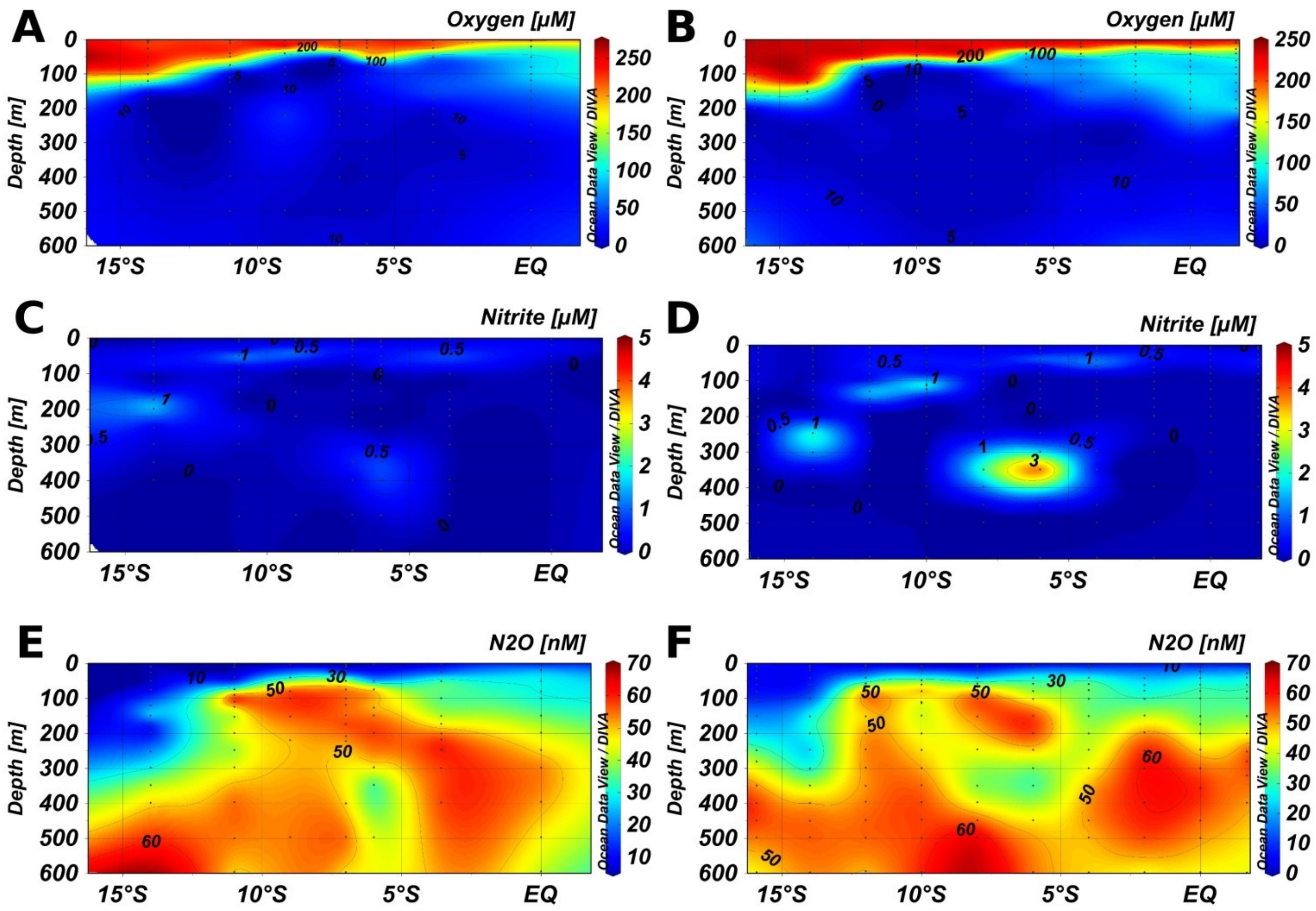

A
Oxygen [µM]
B
Oxygen [µM]
C
Nitrite [µM]
D
Nitrite [µM]
E
N2O [nM]
F
N2O [nM]
Depth [m]
15°S
10°S
5°S
EQ
Ocean Data View / DIVA

Figure 3:

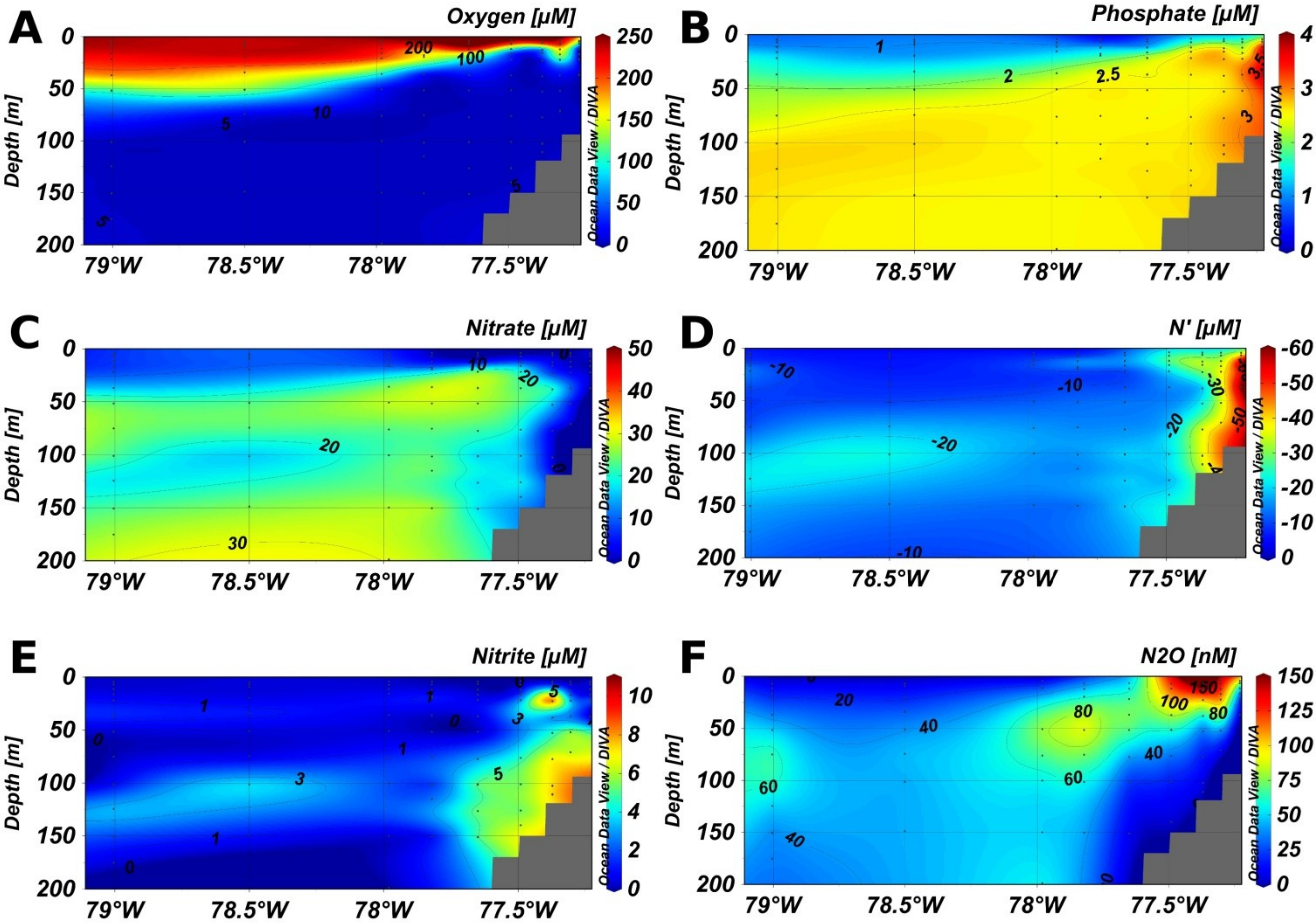
A
Oxygen [µM]
Depth [m]
79°W
78.5°W
78°W
77.5°W
Ocean Data View / DIVA
B
Phosphate [µM]
C
Nitrate [µM]
D
N' [µM]
E
Nitrite [µM]
F
N2O [nM]

Figure 4:

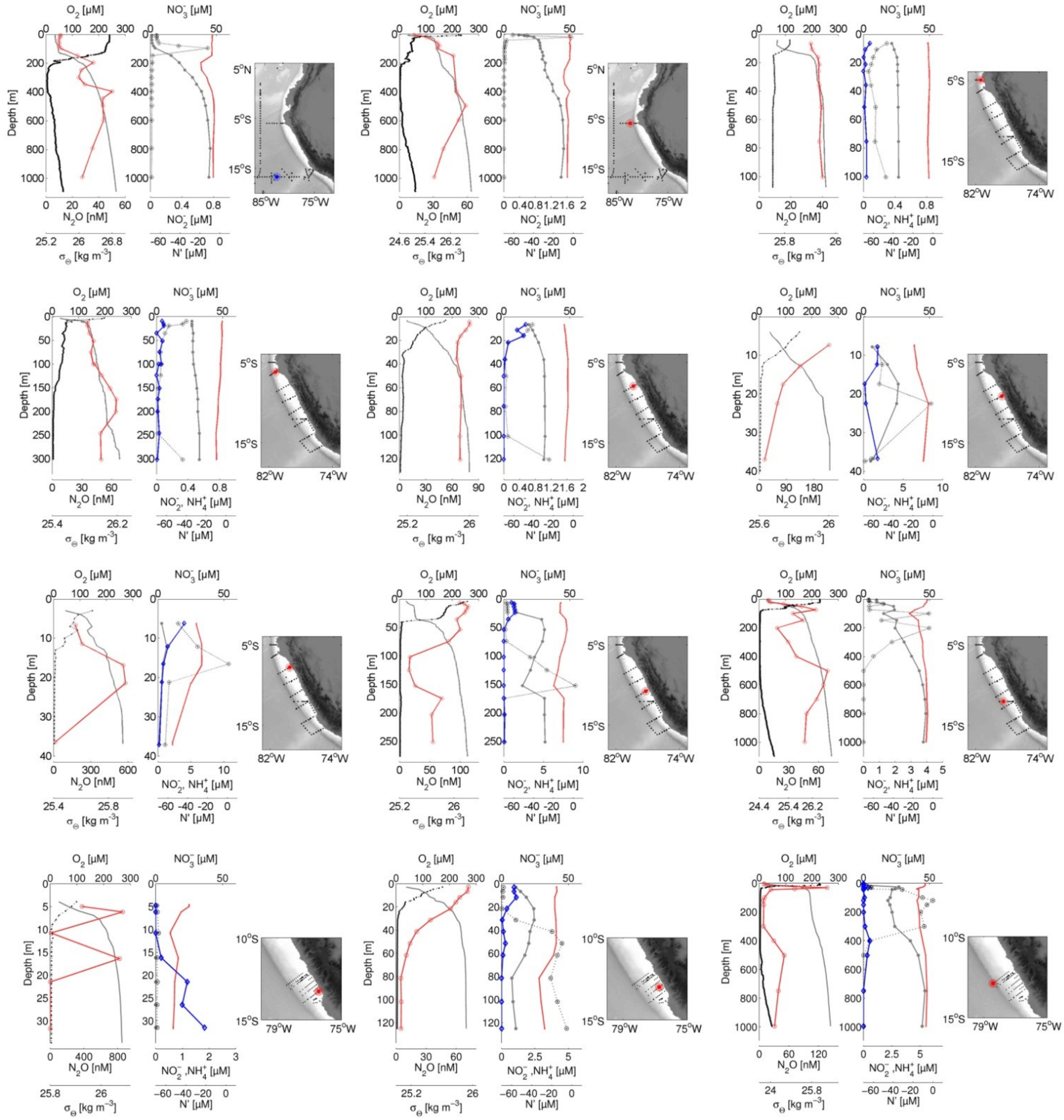

O2 [μM]
NO3- [μM]
Depth [m]
N2O [nM]
NO2- [μM]
NO2-, NH4+ [μM]
σΘ [kg m-3]
N' [μM]
5°N
5°S
10°S
15°S
85°W
75°W
82°W
74°W
79°W

Figure 5:

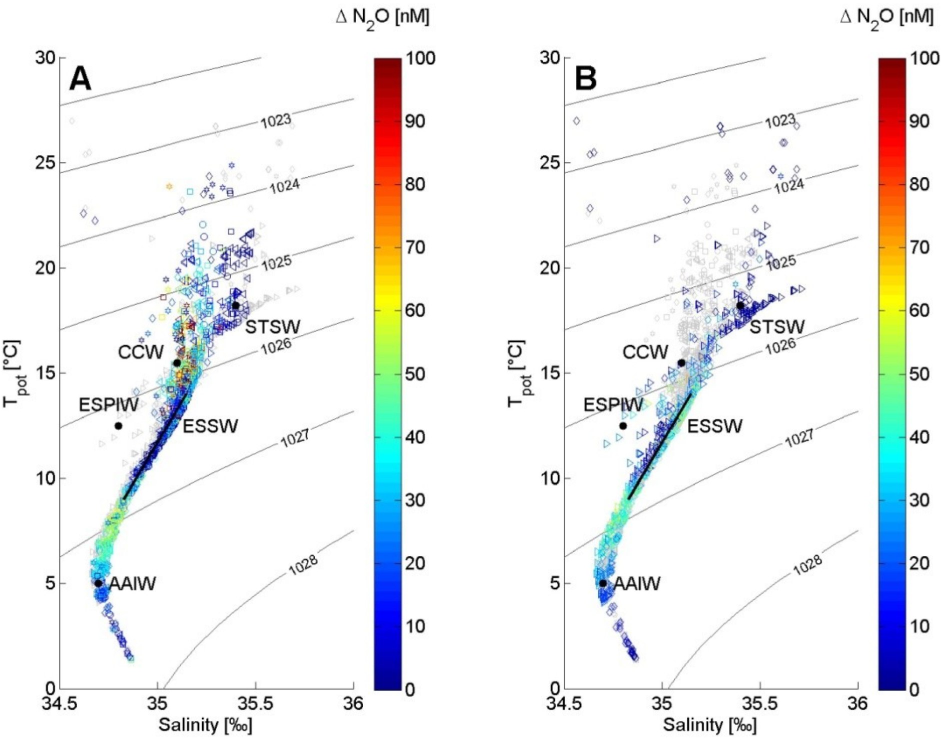

A
B
Δ N2O [nM]
Tpot [°C]
Salinity [‰]
1023
1024
1025
1026
1027
1028
STSW
CCW
ESPIW
ESSW
AAIW

Figure 6:

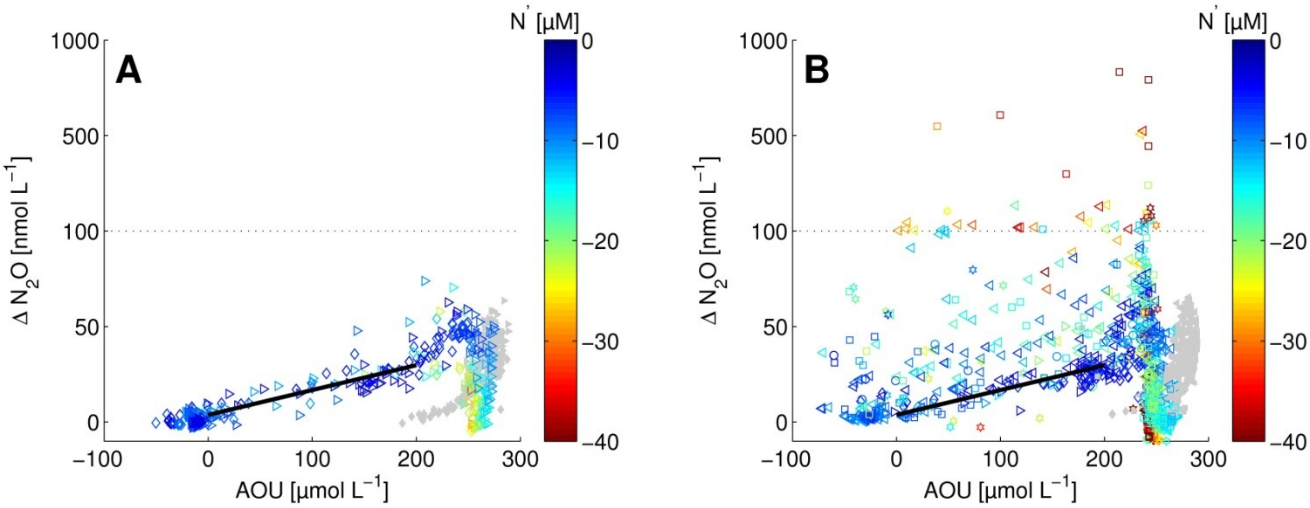
A
B
N' [µM]
Δ N2O [nmol L−1]
AOU [µmol L−1]
1000
500
100
50
0
−100
0
100
200
300
−10
−20
−30
−40